Day-ahead optimal peer-to-peer energy trading strategy for multi-microgrids based on Nash bargaining game with data-driven chance constraints

Boyu Chen[1], Yanbo Che[1], Yue Zhou[2], Shuaijun Zhao[1]
1 Key Laboratory of Smart Grid of Ministry of Education, Tianjin University, Tianjin 300072, China
2 School of Engineering, Cardiff University, Cardiff CF24 3AA, Wales, UK

***Abstract* — This paper proposes an optimization model to obtain the day-ahead optimal peer-to-peer (P2P) trading strategy for multi-microgrids (MMG). Firstly, a joint economic energy and reserve scheduling model of a microgrid (MG) is established while considering specific network constraints. Then, to mitigate the impact of renewable energy and load forecasting errors, chance constraints are introduced for the reserve capacity and buses voltage limitations of an individual microgrid. Additionally, a versatile distribution method is adopted to capture the probability distribution of uncertain variables in a data-driven manner, avoiding any prior assumptions. Finally, Nash bargaining theory is employed to deal with the P2P energy trading problem among MMG. The problem is equivalently transformed into two sequential subproblems for solving. Moreover, the alternating direction method of multipliers algorithm is used to solve the subproblems in a distributed manner for privacy concerns. The proposed model not only enables effective P2P energy trading for MMG, but also ensures compliance with the internal network constraints of each MG. Furthermore, the scheduling strategy exhibits robustness in handling forecast errors related to renewable energy and load. In case studies, MMG containing three interconnected MGs is constructed based on the IEEE-123 bus distribution network, and simulation results show that the cost of the MMG is reduced by 9.92% while all the MGs can benefit from P2P trading. In addition, the risk-averse scheduling results of energy and reserve are obtained, and the conservativeness can be controlled by changing the confidence level, which verifies the effectiveness of the proposed model.**

***Index Terms*-- Multi-microgrids; peer-to-peer energy trading; Nash bargaining game; data-driven chance constraint; distributed optimization.**

Nomenclature

Abbreviations

P2P	Peer-to-peer
MMG	Multi-microgrids
MG	Microgrid
BS	Battery storage
DG	Distributed generator
MILP	Mixed-integer linear programming
SOP	Soft open points
RO	Robust optimization
SO	Stochastic optimization
CCP	Chance constraint programming
PV	Photovoltaic
WT	Wind turbines
MGO	MG operator
PDF	Probability density function
CDF	Cumulative distribution function
ADMM	Alternating direction method of multipliers

Sets

T	Set of time slots
G	Set of DG
BS	Set of BS
$\mathcal{B}$	Set of buses

Indices

t	Indexes of time slots
g	Indexes of DG
bs	Indexes of BS
j	Indexes of buses

Variables

$P_t^{gd,b}$	Buying power from the main grid
$P_t^{gd,s}$	Selling power to the main grid
P_t^{g}	Output power of controllable DG
x_t^{g}	Binary variable indicates the operating status of DG
$x_t^{g,su}$, $x_t^{g,dn}$	Binary variable indicating the starting and stopping status of DG, respectively
$R_t^{g,dn}$, $R_t^{g,up}$	Downward and upward reserve of DG
E_t^{bs}	Energy state of BS
$P_t^{bs,c}$, $P_t^{bs,d}$	Charging and discharging power of BS
$R_t^{bs,dn}$, $R_t^{bs,up}$	Downward and upward reserve of BS
Q_t^{gd}	Interactive reactive power between MG and the main grid

Boyu Chen and Shuaijun Zhao are with the Key Laboratory of Smart Grid of Ministry of Education, Tianjin University, Tianjin 300072, China (e-mail: bychen@tju.edu.cn; zhaoshuaijun2021@tju.edu.cn).

Yue Zhou is with the School of Engineering, Cardiff University, Cardiff CF24 3AA, Wales, UK (e-mail: ZhouY68@cardiff.ac.uk).

Corresponding author: Yanbo Che is with the Key Laboratory of Smart Grid of Ministry of Education, Tianjin University, Tianjin 300072, China (e-mail: lab538@163.com).

P_{jt}^{in}	Injected active power of the bus j
Q_{jt}^{in}	Injected reactive power of the bus j
V_{jt}	Voltage amplitude of the bus j
$P_{ij,t}^{l}$	Active power on the branch l
$Q_{ij,t}^{l}$	Reactive power on the branch l
$P_{m,t}^{n}$	Active power trading from MG m to MG n
$Q_{m,t}^{n}$	Reactive power supporting by SOP to MG m
$P_{m,t}^{n,loss}$	Active power loss of SOP

Parameters

pr_t^b	Buying price of electricity
pr_t^s	Selling price of electricity
a_g, b_g, c_g	Cost factors of the DG
$pr^{g,su}$, $pr^{g,dn}$	Starting and stopping costs of DG
$\underline{P}^g$, $\overline{P}^g$	Lower and upper output limits of DG
η^c, η^d	Charging and discharging efficiency of BS
$\overline{E}^{bs}$, $\underline{E}^{bs}$	Upper and lower limits of the energy state
E_0^{bs}	Initial energy state of BS
$\overline{P}^{bs,c}$, $\overline{P}^{bs,d}$	Upper limit of charging power and discharging power
$\overline{P}^{gd}$	Maximum interactive active interactive power between MG and the main grid
$\overline{Q}^{gd}$	Maximum interactive reactive power between MG and the main grid
κ_j	Binary parameter indicating the connection status of the bus to the equipment
$\overline{P}_{ij}^{l}$	Upper limits of active power of the branch
$\overline{Q}_{ij}^{l}$	Upper limits of reactive power of the branch
V_0	Voltage amplitude of the root bus
$\Delta\overline{V}$	Maximum allowable deviation of the bus voltage
A^{sop}	Loss factor of SOP
$S_m^{n,sop}$	Capacity of SOP

1. Introduction

Distributed generators (DG), battery storage (BS), and local loads can be integrated into a microgrid (MG) for efficient management [1]. With the increasing penetration of distributed energy resources, multiple interconnected MGs, will emerge in the neighborhood to form the multi-microgrids (MMG) [2]. The concept of the control system of MMG was first introduced in [3]. MMG can take advantage of the differentiated resource distribution and supply-demand relationship between different MGs to achieve power supply through peer-to-peer (P2P) trading, reduce total system operating costs, and improve operational reliability [4]. In MMG, each MG is a profit-seeker, usually aiming to reduce its own operating costs [5]. Therefore, reasonable MMG scheduling strategy and trading mechanisms are needed to incentivize MGs to participate in P2P trading and achieve win-win cooperation among all the MGs [6].

1.1. Related work and motivation

The scheduling framework for the P2P transaction of MMG can be classified as centralized or decentralized. The centralized scheduling framework requires a central controller that collects detailed information about each MG and develops the scheduling strategy for all the MGs in MMG [7], [8]. Ref. [9] considers mobile energy storage when formulating P2P trading strategies for MMG, while Ref. [10] takes demand-side response into account. A cooperative game model for MMG was developed in [11], and the economic benefits were assigned to each MG using Shapely values. Ref. [12] presented a bi-level energy management framework to coordinate P2P energy trading among multiple prosumers. By using Karush-Kuhn-Tucker conditions, the bi-level model was transformed into an equivalent single-level mixed-integer linear programming (MILP) problem for solving.

However, in the aforementioned studies, when employing a manager to facilitate energy sharing between MGs within a centralized scheduling framework, several drawbacks emerge. Firstly, this approach necessitates each MG to disclose detailed information regarding its internal devices, thereby compromising the data privacy of the MG. Secondly, it imposes rigorous demands on communication and control systems, resulting in a lack of scalability and potentially burdening the computational resources [13], [14]. Due to the privacy concerns associated with each microgrid, using a centralized scheduling framework in practical applications can be challenging. In contrast to the above studies, a decentralized scheduling framework for P2P energy trading of MMG had been established based on distributed algorithms such as the analytical target cascading algorithm [15], alternating direction method of multipliers (ADMM) algorithm [16], [17], [18], [19], and Dantzig-Wolfe decomposition algorithm [20]. In the decentralized scheduling framework, each MG only needs to utilize optimization model decomposition techniques and share limited information with neighboring MGs or a third-party coordinator, such as the exchanged power between other MGs. The detailed data of renewable energy generation, load power, power network topology, and other internal information within each MG is kept private, achieving the scheduling independence of MGs.

In peer-to-peer energy trading, it is essential to consider the interests of different participants and develop a fair and reasonable energy trading clearance mechanism. Cooperative game theory is a widely adopted approach to achieving this objective. A cooperative game model for MMG was developed in [11], and the economic benefits of collaborative scheduling were assigned to each MG using Shapely values. However, in situations where a large number of players are involved, the computational complexity of this method becomes a significant obstacle. To overcome this challenge,

researchers have turned to Nash bargaining theory as an alternative model for cooperative energy trading problems. In [18] and [21], the Nash bargaining game optimization model was established for the coordinated operation problem of MMG, while considering demand side management. Ref. [22] proposed a bi-level P2P multi-energy trading framework and the lower-level P2P energy market was settled using Nash bargaining theory. Nash bargaining optimization model can be equivalently transformed into a social welfare optimization problem and a payment bargaining problem subproblem. These subproblems can then be solved within a distributed scheduling framework [16].

In [7]–[12] and [15]–[19], MGs were approximately simplified as aggregation buses, which lacks the consideration of the internal topology of MGs. This may cause the optimal scheduling strategy to violate physical constraints of power networks in MGs, making the strategy unfeasible. With the increasing penetration of renewable power generation and electric vehicles, over-voltage and under-voltage problems are becoming more and more prominent. It is essential to consider the network constraints within MG. In recent years, soft open points (SOP) have been widely used in distribution networks to replace traditional contact switches. When the SOP is installed between different feeder buses, it can effectively control the active power transmission between feeders while also providing reactive power support [23]. Therefore, by using SOPs to connect MGs, flexible connection of multiple MGs and complete controllability of power flow between MGs can be achieved. It provides an effective interconnection between MGs at physical level [24].

In addition, there are significant uncertainties in load consumption and renewable generation. Robust optimization (RO) [11], [20], [25], [26] and stochastic optimization (SO) [12], [18], [20] are two common methods to deal with uncertainty. RO only requires the boundary values of uncertain variables, but it will result in over-conservative scheduling results. SO uses information about the probability distribution of uncertain variables to generate multiple stochastic scenarios, resulting in robustness of the scheduling results being dependent on the generated stochastic scenarios and the computational complexity growing exponentially with the number of scenarios.

The chance constraint programming (CCP) is another effective approach to deal with uncertain variables, which allows the constraints to be violated with a small probability. CCP is more appropriate to be applied in decentralized dispatch because of the less computational burden compared to SO, and the conservativeness of the solution can be controlled by changing the confidence level. In previous studies, CCP was widely used in the scheduling problem of integrated energy systems [27], MGs [28], active distribution networks [29], and MMG [15]. CCP requires prior knowledge about the probability distribution information of uncertain variables, which has traditionally been assumed to follow a Gaussian distribution in previous studies. However, the assumed probability distributions may not be well suited to real-world situations. If the actual distribution of prediction errors deviates from the Gaussian assumption, the resulting scheduling outcomes may fail to meet the confidence requirements of chance constraints, leading to violations of the operational constraints of the system and compromising its safety and stability. Fortunately, with the advancement of advanced measurement technologies, it has become feasible to extract probability distribution characteristics of prediction errors in a data-driven manner using historical measurement data. By employing a probability distribution that better aligns with the actual prediction error distribution, these issues can be mitigated.

1.2. Objective and contributions

There are two main issues in developing an optimal P2P trading strategy for MMG: 1) how to develop a dispatch strategy for each MG and 2) how to trade energy with other MGs and distribute the benefits. This paper aims to formulate an optimization model to obtain the day-ahead optimal P2P trading strategy for MMG, which can effectively solve the above two issues. In each MG, the network constraints are considered, and load consumption and renewable generation uncertainties are dealt with by a data-driven CCP approach. The P2P optimization model for maximizing the total benefits of MMG is established based on the Nash bargaining game theory and solved in a distributed manner. The comparison of the research between this paper and the previous studies is shown in Table 1.

Table 1

Comparison of the research of this paper and previous studies.

Paper	Network Constraints	Decentralized	Nash bargaining	Uncertainty			
				RO	SO	CCP	Data-driven CCP
[7][8][9][10]					√		
[11]				√			
[12]			√		√		
[13][14]	√				√		
[15]		√				√	
[16][17]		√	√				
[18]		√	√		√		
[19]		√					
[20]	√	√		√	√		
[21]		√	√	√			
[22]	√	√	√				
[25]	√			√			
[26]	√	√	√	√			
This paper	√	√	√				√

The main contributions of this paper are summarized as follows.

(1) This paper considers the internal power flow constraints and establishes a joint energy and reserve economic dispatch model for an individual microgrid. CCP is used to handle the impact of renewable energy forecasting errors on reserve capacity and bus voltage limits. Unlike previous studies that assumed the forecasting errors followed a Gaussian distribution, this paper uses a versatile distribution to characterize the probability distribution of forecasting errors. The parameters of this versatile distribution are obtained in a data-driven manner using historical forecasting error data, avoiding the need to assume a specific probability distribution for forecasting errors.

(2) In this paper, MGs are connected via SOPs to construct MMG. Over-voltage and under-voltage problems of MGs are tackled by the reactive power output from SOPs. The Nash bargaining model is established for the P2P trading of MMG. Two sequential subproblems, equivalent to the Nash bargaining model, are formulated as a mixed-integer second-order cone programming (MISOCP) and a convex optimization problem, respectively. The optimization models of the subproblems are solved in a distributed manner using the ADMM algorithm.

(3) MMG containing three MGs are constructed based on the IEEE 123-bus distribution network for simulation. First, the fitting effect of the versatile distribution is verified. Then, the dispatching results of energy and reserve and the operating cost of MMG are analyzed to verify the effectiveness of the proposed method. Finally, the influence of the confidence level on the scheduling results is analyzed.

The remainder of this paper is organized as follows. The optimization model of MGs with chance constraints is developed in Section 2. In Section 3, the Nash bargaining model of MMG is established, and the solution method is proposed. The results and analysis of the case study are presented in Section 4. Finally, this study is summarized with the future research topics discussed in Section 5.

2. Chance constrained optimization model of an individual microgrid

2.1. Optimization framework of an individual microgrid

The optimization framework of an individual MG proposed in the paper is shown in Fig. 1. Renewable generation like photovoltaic (PV) panels and wind turbines (WT), as well as controllable DGs, are used to satisfy the load demand in the MG. The MG can also buy electricity from the main grid or sell surplus electricity to the main grid while operating in the grid-connected mode. In addition, BSs can provide additional dispatch flexibility for the MG. The MG operator (MGO) is responsible for developing the day-ahead dispatch plan for the MG. The versatile distribution is used to model the probability distribution of forecast errors, and chance constraints are formulated based on the versatile distribution. The MG is considered as a controllable entity in which the forecast error can be balanced by scheduling the reserve. According to the next day's power forecast curves, energy and reserve day-ahead dispatch plans of DGs and BSs are developed by solving the optimization model.

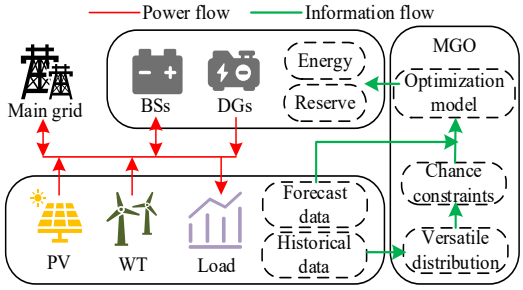

Fig. 1. The illustration of the proposed MG optimization framework.

2.2. Objective function

The MGO aims to minimize its operating costs, including the cost of interaction with the main grid and the fuel cost of controllable generators. The objective function can be expressed as:

$$\min \quad C_{mg}=\sum_{t\in \mathrm{T}}\left(\begin{array}{l}\mathrm{pr}_{\mathrm{t}}^{\mathrm{b}} P_t^{gd,b}-\mathrm{pr}_{\mathrm{t}}^{\mathrm{s}} P_t^{gd,s}+\mathrm{a}_{\mathrm{g}} P_t^{g2}+\\ \mathrm{b}_{\mathrm{g}} P_t^{g}+\mathrm{c}_{\mathrm{g}}+\mathrm{pr}^{\mathrm{g,su}} x_t^{g,su}+\mathrm{pr}^{\mathrm{g,dn}} x_t^{g,\mathrm{dn}}\end{array}\right) \tag{1}$$

The quadratic function about the operating cost of DGs can be linearized using the piecewise linearization method [30].

2.3. Constraints

(1) Distributed generator constraints

In the day-ahead stage, the output power and reserve capacity are scheduled and should satisfy the power limitation constraints. The reactive power of DGs is not considered in the paper, i.e., the power factor of DGs is 1. The constraints of DGs are shown as follows:

$$\underline{\mathrm{P}}^{\mathrm{g}} x_t^g+R_t^{g,dn}\le P_t^g\le \overline{\mathrm{P}}^{\mathrm{g}} x_t^g-R_t^{g,up} \qquad \forall g\in \mathrm{G} \tag{2}$$

$$x_t^{g,su}-x_t^{g,dn}=x_t^g-x_{t-1}^g \qquad \forall g\in \mathrm{G} \tag{3}$$

$$R_t^{g,dn}\ge 0,\ \ R_t^{g,up}\ge 0 \qquad \forall g\in \mathrm{G} \tag{4}$$

(2) Battery storage constraints

The charging, discharging power, and reserve capacity of BSs are also scheduled at the day-ahead stage. The constraints are shown as follows:

$$E_t^{bs}=E_{t-1}^{bs}+\left(\eta^{\mathrm{c}} P_t^{bs,c}-P_t^{bs,d}/\eta^{\mathrm{d}}\right)\Delta \mathrm{t} \quad \forall bs\in \mathrm{BS} \tag{5}$$

$$\underline{\mathrm{E}}^{\mathrm{bs}}\le E_t^{bs}\le \overline{\mathrm{E}}^{\mathrm{bs}},\ \ E_T^{bs}=\mathrm{E}_0^{\mathrm{bs}} \qquad \forall bs\in \mathrm{BS} \tag{6}$$

$$P_t^{bs,c}+R_t^{bs,dn}\le \overline{\mathrm{P}}^{\mathrm{bs,c}},\ R_t^{bs,dn}\le \overline{\mathrm{P}}^{\mathrm{bs,c}}+P_t^{bs,d} \quad \forall bs\in \mathrm{BS} \tag{7}$$

$$P_t^{bs,d}+R_t^{bs,up}\le \overline{\mathrm{P}}^{\mathrm{bs,d}},\ \ R_t^{bs,up}\le \overline{\mathrm{P}}^{\mathrm{bs,d}}+P_t^{bs,c} \quad \forall bs\in \mathrm{BS} \tag{8}$$

$$P_t^{bs,c}\ge 0,\ \ P_t^{bs,d}\ge 0,\ \ R_t^{bs,dn}\ge 0,\ \ R_t^{bs,up}\ge 0 \quad \forall bs\in \mathrm{BS} \tag{9}$$

(3) Main grid constraints

The active and reactive power interaction between the MG and the main grid should meet the upper and lower limits, as follows:

$$0 \le P_t^{gd,b} \le \overline{\mathrm{P}}^{\mathrm{gd}},\ 0 \le P_t^{gd,s} \le \overline{\mathrm{P}}^{\mathrm{gd}} \tag{10}$$

$$-\overline{\mathrm{Q}}^{\mathrm{gd}} \le Q_t^{gd} \le \overline{\mathrm{Q}}^{\mathrm{gd}} \tag{11}$$

(4) Network constraints

In this paper, the power flow of MGs is modeled using the linearized DistFlow model [31], [32], which can be expressed as:

$$P_{jt}^{in} = \begin{pmatrix} \kappa_{\mathrm{j}}^{\mathrm{gd}}(P_t^{gd,b} - P_t^{gd,s}) + \kappa_{\mathrm{j}}^{\mathrm{g}} P_t^{g} + \kappa_{\mathrm{j}}^{\mathrm{pv}} P_t^{pv} + \\ \kappa_{\mathrm{j}}^{\mathrm{wt}} P_t^{wt} + \kappa_{\mathrm{j}}^{\mathrm{bs}}(P_t^{bs,d} - P_t^{bs,c}) - \kappa_{\mathrm{j}}^{\mathrm{ld}} P_t^{ld} \end{pmatrix} \quad \forall j \in \mathcal{B} \tag{12}$$

$$Q_{jt}^{in} = \kappa_{\mathrm{j}}^{\mathrm{gd}} Q_t^{gd} - \kappa_{\mathrm{j}}^{\mathrm{ld}} Q_{jt}^{ld} \quad \forall j \in \mathcal{B} \tag{13}$$

$$P_{jt}^{in} = \sum_{k \in \varphi(\mathrm{j})} P_{jk,t}^{l} - \sum_{i \in \theta(\mathrm{j})} P_{ij,t}^{l} \quad \forall j \in \mathcal{B} \tag{14}$$

$$Q_{jt}^{in} = \sum_{k \in \varphi(\mathrm{j})} Q_{jk,t}^{l} - \sum_{i \in \theta(\mathrm{j})} Q_{ij,t}^{l} \quad \forall j \in \mathcal{B} \tag{15}$$

$$V_{it} - V_{jt} = \left(P_{ij,t}^{l} \mathrm{r}_{\mathrm{ij}} + Q_{ij,t}^{l} \mathrm{x}_{\mathrm{ij}}\right) \Big/ \mathrm{V}_0 \quad \forall l \in \ell \tag{16}$$

$$-\overline{\mathrm{P}}_{\mathrm{ij}}^{\mathrm{l}} \le P_{ij,t}^{l} \le \overline{\mathrm{P}}_{\mathrm{ij}}^{\mathrm{l}} \quad \forall l \in \ell \tag{17}$$

$$-\overline{\mathrm{Q}}_{\mathrm{ij}}^{\mathrm{l}} \le Q_{ij,t}^{l} \le \overline{\mathrm{Q}}_{\mathrm{ij}}^{\mathrm{l}} \quad \forall l \in \ell \tag{18}$$

$$\mathrm{V}_0 - \Delta\overline{\mathrm{V}} \le V_{jt} \le \mathrm{V}_0 + \Delta\overline{\mathrm{V}} \quad \forall j \in \mathcal{B} \tag{19}$$

2.4. Uncertain variables model

In the above optimization model, the renewable generation and load consumption are difficult to predict accurately. They are uncertain variables, which can be expressed as the sum of the forecast value and the forecast error:

$$\tilde{P}^{uv} = P^{uv,f} + \xi^{uv} \tag{20}$$

where $P^{uv,f}$ and ξ^{uv} denote the forecast value and forecast errors of uncertain variables, respectively. The superscripts uv represents PV, WT, or load.

When using CCP to address uncertain variables in MGs, the probability distribution of the forecast error needs to be determined first. In previous studies, the forecast errors were assumed to follow Gaussian distribution. However, this assumption may not be well guaranteed in reality. Hence, this paper uses a versatile distribution to model the probability distribution of forecast errors [33]. This method is data-driven, and the distribution information can be obtained from historical data without prior assumptions. The probability density function (PDF), the cumulative distribution function (CDF), and the inverse function of the CDF of the versatile distribution can be expressed as:

$$f(\xi^{uv}) = \frac{\delta\beta e^{-\delta(\xi^{uv}-\gamma)}}{\left(1+e^{-\delta(\xi^{uv}-\gamma)}\right)^{\beta+1}} \tag{21}$$

$$F(\xi^{uv}) = \left(1+e^{-\delta(\xi^{uv}-\gamma)}\right)^{-\beta} \tag{22}$$

$$F_{\xi^{uv}}^{-1}(\varepsilon) = \gamma - \frac{1}{\delta}\ln\left(c^{-1/\beta}-1\right) \tag{23}$$

where δ, β and γ are the shape parameters, and ε is a parameter related to the confidence level. The nonlinear least-squares fitting method can be used to determine the shape parameters based on historical data. Since the shape parameters are obtained in a data-driven way based on historical data, the versatile distribution endogenously reflects the uncertain level of the uncertain variables without any prior assumptions. Leveraging the Eq. (23), the upper and lower bounds of the forecast error can be determined with the value of ε specified by the MGO. In addition, it can be seen from Eq. (23) that the inverse function of the CDF has an exact analytical form. Thus, the chance constraints constructed based on the versatile distribution can be easily reformulated into a solvable form.

2.5. Chance constraints model

CCP is a commonly used method for handling uncertain variables. It achieves risk-averse scheduling outcomes by ensuring that the probability of meeting specific constraints is at least as high as a specified confidence level. For ease of comprehension, the general form of chance constraints can be represented as: $\mathbb{P}_\theta\left(g(x,\theta) \le 0\right) \ge 1-\varepsilon$. $g(x,\theta)$ represents the constraint function that depends on both the decision variable x and the uncertain parameter θ. The inequality $g(x,\theta) \le 0$ represents the constraint to be satisfied. The parameter ε represents the allowed violation probability, and the term $1-\varepsilon$ denotes the confidence level, indicating the desired probability of meeting the constraint. A higher confidence level indicates that a higher uncertainty level is considered, and the chance constraint will be satisfied with a higher probability. Notably, a smaller probability of violation corresponds to a more conservative optimal scheduling, which brings more operating costs to MGOs. Hence, the MGO can control the conservatism of the optimal scheduling results by choosing an appropriate value of confidence level and making a trade-off between the conservatism and the economy of the optimal scheduling.

In this paper, the total forecast error ξ_t of uncertain variables in MGs can be expressed as:

$$\xi_t = \sum_{wt \in \mathrm{WT}} \xi_t^{wt} + \sum_{pv \in \mathrm{PV}} \xi_t^{pv} - \sum_{ld \in \mathrm{LD}} \xi_t^{ld} \tag{24}$$

A linear affine strategy is used to assign the total forecast error to the controllable units within the MG. $\alpha_t^{g,up}$ and $\alpha_t^{g,dn}$ denote the upward and downward reserve affine coefficients of DGs in time slot t, respectively. $\alpha_t^{bs,up}$ and $\alpha_t^{bs,dn}$ denote the upward and downward reserve affine coefficients of BSs in time slot t, respectively. The constraints of reserve affine coefficients can be expressed as:

$$\alpha_t^{g,up} \ge 0,\ \alpha_t^{bs,up} \ge 0,\ \sum_{g \in \mathrm{G}} \alpha_t^{g,up} + \sum_{bs \in \mathrm{BS}} \alpha_t^{bs,up} = 1 \tag{25}$$

$$\alpha_t^{g,dn} \ge 0,\ \alpha_t^{bs,dn} \ge 0,\ \sum_{g \in \mathrm{G}} \alpha_t^{g,dn} + \sum_{bs \in \mathrm{BS}} \alpha_t^{bs,dn} = 1 \tag{26}$$

To meet the reserve demand with a significant probability, chance constraints are added to the upward and downward reserve provided by DGs and BSs as shown in Eqs. (27) and (28).

$$\mathbb{P}_{\xi_t}\left(-R_t^{g,dn} \le \alpha_t^{g,dw}\xi_t\ , \alpha_t^{g,up}\xi_t\ \le R_t^{g,up}\right) \ge 1-\varepsilon \quad \forall g \in \mathrm{G} \tag{27}$$

$$\mathbb{P}_{\xi_t}\left(-R_t^{bs,dn} \le \alpha_t^{bs,dn}\xi_t\,, \alpha_t^{bs,up}\xi_t \le R_t^{bs,up}\right) \ge 1-\varepsilon \quad \forall bs \in \mathrm{BS} \tag{28}$$

where ε is a small positive number, indicating that the reserve demand is satisfied at the confidence level of $1-\varepsilon$.

Forecast errors also impact not only the line power but also the bus voltage in MGs. While branches in MGs are typically not congested, problems related to over-voltage and under-voltage violations tend to occur at several buses [34], [35]. As a result, the chance constraint for limiting bus voltage can be expressed as:

$$\mathbb{P}_{\xi_t}\left(\mathrm{V}_0 - \Delta\overline{\mathrm{V}} \le v_{jt}(\xi_t^{wt},\xi_t^{pv},\xi_t^{ld}) \le \mathrm{V}_0 + \Delta\overline{\mathrm{V}}\right) \ge 1-\varepsilon \quad \forall j \in \mathcal{B} \tag{29}$$

where $v_{jt}(\xi_t^{wt},\xi_t^{pv},\xi_t^{ld})$ is a function which represents the relationship between the bus voltage and forecast errors. Since the network structure of MGs is radial and the power flow equations are linear, there is a linear relationship between bus voltage and bus injected power, i.e., $v_{jt}(\xi_t^{wt},\xi_t^{pv},\xi_t^{ld})$ is a linear function.

In the chance constraints, the confidence levels for satisfying the upper and lower limits are specified as $1-\varepsilon/2$. Based on the inverse function of the CDF in Eq. (23) and the linear property of function $v_{jt}(\xi_t^{wt},\xi_t^{pv},\xi_t^{ld})$, chance constraints (27) – (29) can be reformulated as Eqs. (30) – (37) [36].

$$-R_t^{g,dn} \le \alpha_t^{g,dn}(\underline{\xi}_t^{ld} - \overline{\xi}_t^{wt} - \overline{\xi}_t^{pv}) \quad \forall g \in \mathrm{G} \tag{30}$$

$$R_t^{g,up} \ge \alpha_t^{g,up}(\overline{\xi}_t^{ld} - \underline{\xi}_t^{wt} - \underline{\xi}_t^{pv}) \quad \forall g \in \mathrm{G} \tag{31}$$

$$-R_t^{bs,dn} \le \alpha_t^{bs,dn}(\underline{\xi}_t^{ld} - \overline{\xi}_t^{wt} - \overline{\xi}_t^{pv}) \quad \forall bs \in \mathrm{BS} \tag{32}$$

$$R_t^{bs,up} \ge \alpha_t^{bs,up}(\overline{\xi}_t^{ld} - \underline{\xi}_t^{wt} - \underline{\xi}_t^{pv}) \quad \forall bs \in \mathrm{BS} \tag{33}$$

$$\mathrm{V}_0 - \Delta\overline{\mathrm{V}} \le v_{jt}(\underline{\xi}_t^{ld},\underline{\xi}_t^{pv},\underline{\xi}_t^{wt}) \le \mathrm{V}_0 + \Delta\overline{\mathrm{V}} \quad \forall j \in \mathcal{B} \tag{34}$$

$$\mathrm{V}_0 - \Delta\overline{\mathrm{V}} \le v_{jt}(\underline{\xi}_t^{ld},\overline{\xi}_t^{pv},\overline{\xi}_t^{wt}) \le \mathrm{V}_0 + \Delta\overline{\mathrm{V}} \quad \forall j \in \mathcal{B} \tag{35}$$

$$\mathrm{V}_0 - \Delta\overline{\mathrm{V}} \le v_{jt}(\overline{\xi}_t^{ld},\underline{\xi}_t^{pv},\underline{\xi}_t^{wt}) \le \mathrm{V}_0 + \Delta\overline{\mathrm{V}} \quad \forall j \in \mathcal{B} \tag{36}$$

$$\mathrm{V}_0 - \Delta\overline{\mathrm{V}} \le v_{jt}(\overline{\xi}_t^{ld},\overline{\xi}_t^{pv},\overline{\xi}_t^{wt}) \le \mathrm{V}_0 + \Delta\overline{\mathrm{V}} \quad \forall j \in \mathcal{B} \tag{37}$$

where $\underline{\xi}_t^{ld}$ and $\overline{\xi}_t^{ld}$ are the lower and upper bounds of forecast error of load consumption, respectively; $\underline{\xi}_t^{pv}$ and $\overline{\xi}_t^{pv}$ are the lower and upper bounds of forecast error of the PV generation, respectively; $\underline{\xi}_t^{wt}$ and $\overline{\xi}_t^{wt}$ are the lower and upper bounds of forecast error of the WT generation, respectively. Based on the inverse function of the CDF of the versatile distribution, the lower and upper bounds of the forecast errors can be calculated as follows:

$$\underline{\xi}_t^{ld} = F_{\xi_t^{ld}}^{-1}(\varepsilon/2),\ \overline{\xi}_t^{ld} = F_{\xi_t^{ld}}^{-1}(1-\varepsilon/2) \tag{38}$$

$$\underline{\xi}_t^{pv} = F_{\xi_t^{pv}}^{-1}(\varepsilon/2),\ \overline{\xi}_t^{pv} = F_{\xi_t^{pv}}^{-1}(1-\varepsilon/2) \tag{39}$$

$$\underline{\xi}_t^{wt} = F_{\xi_t^{wt}}^{-1}(\varepsilon/2),\ \overline{\xi}_t^{wt} = F_{\xi_t^{wt}}^{-1}(1-\varepsilon/2) \tag{40}$$

It is worth noting that compared with CCP when using RO to deal with uncertain variables, the obtained scheduling results are over-conservative since the information on the probability distribution is not considered. Although the conservativeness of the optimal scheduling results can be controlled by the uncertainty budget in RO [37], the probability of violating the reserve and bus voltage constraints still cannot be directly quantified. Moreover, when using RO, the duality process should be conducted, which adds additional auxiliary variables and increase the complexity of the optimization model. In SO, the objective is to minimize the average operating costs with the scenarios considered [38], [39]. Hence, the obtained optimal scheduling result is essentially a risk-neutral scheduling result. By contrast, in this paper, leveraging CCP, the MGO can obtain risk-averse scheduling, effectively hedging against the operating risk caused by forecast errors. In addition, scenario-based SO provides poor out-of-sample performance unless the number of scenarios is very high, which in turn increases the computational burden. When using SO, scenario reduction is generally necessary. However, finding the optimal compromise between out-of-sample performance and calculation efficiency is not easy. Hence, in this paper, by using CCP, the probabilities of violating the reserve and bus voltage constraints are quantified leveraging the probability distribution information of versatile distribution, and the risk-averse scheduling results, which can satisfy the chance constraints at a probability more than the predefined level, are obtained. In addition, the lower model complexity of CCP can well accommodate the calculation efficiency requirement when the optimization model needs to be solved repeatedly within a decentralized scheduling framework.

Ultimately, the economic scheduling optimization problem with chance constraints for a single MG can be formulated as a MILP as follows:

$$\begin{aligned} &\text{obj} \quad (1) \\ &\text{s.t.} \quad (2)-(19),\ (24)-(26),\ (30)-(40) \end{aligned} \tag{41}$$

3. Nash bargaining model of MMG and solution method

3.1. Nash bargaining model for MMG

The Nash bargaining solution satisfies a set of axioms, including symmetry, where indistinguishable agents receive the same amount of profit, and Pareto optimality, where an agent's profit cannot be increased unless at least one other agent's profit is decreased. In Nash bargaining, the profit allocation can establish cooperation among agents by guaranteeing that each agent has a higher profit than it does in a noncooperative case. Using the Nash bargaining game approach, minimizing the operating costs of MMG, i.e., maximizing social welfare, is achieved. The benefits obtained from P2P energy trading are also rationally distributed among the MGs. The Nash bargaining game model is formulated as Eq. (42). $C_{mg}^{m,\mathrm{co}}$ denote the operating costs of the MG m after the bargaining process. If microgrids cannot reach an agreement, the bargaining process breaks down, and MG m will operate individually with the operating cost $C_{mg}^{m,\mathrm{ind}}$.

It is also referred to as the disagreement point in the Nash bargaining game.

$$\begin{aligned} &\max \prod_{m=1}^{\mathrm{M}}\left(C_{mg}^{m,\mathrm{ind}}-C_{mg}^{m,\mathrm{co}}\right) \\ &\text{s.t. } C_{mg}^{m,\mathrm{ind}}-C_{mg}^{m,\mathrm{co}}\geq 0 \end{aligned} \tag{42}$$

where M denotes the number of MGs participating in the Nash bargaining game. By solving the above optimization problem, the optimal P2P trading strategy of MMG can be obtained.

The above Nash bargaining model can be equivalently decomposed into two sequential subproblems [40]. The first subproblem is the P2P trading problem to minimize the operating cost of MMG and obtain the optimal P2P trading strategy. The second subproblem is the payment bargaining problem to achieve a reasonable distribution of total benefits among MGs.

(1) SP1: P2P energy trading problem

The constraints of SOPs should be satisfied in the P2P trading problem, which can be expressed as follows:

$$P_{m,t}^{n}+P_{m,t}^{\mathrm{loss}}+P_{n,t}^{m}+P_{n,t}^{\mathrm{loss}}=0 \tag{43}$$

$$-\overline{\mathrm{Q}}_{\mathrm{m}}^{\mathrm{n,sop}}\leq Q_{m,t}^{n}\leq \overline{\mathrm{Q}}_{\mathrm{m}}^{\mathrm{n,sop}} \tag{44}$$

$$P_{m,t}^{\mathrm{loss}}=\mathrm{A}^{\mathrm{sop}}\sqrt{\left(P_{m,t}^{n}\right)^{2}+\left(Q_{m,t}^{n}\right)^{2}} \tag{45}$$

$$\sqrt{\left(P_{m,t}^{n}\right)^{2}+\left(Q_{m,t}^{n}\right)^{2}}\leq \mathrm{S}_{\mathrm{m}}^{\mathrm{n,sop}} \tag{46}$$

Eqs. (45) and (46) can be reformulated to second-order cone constraints (47) and (48), respectively [41].

$$\left(P_{m,t}^{n}\right)^{2}+\left(Q_{m,t}^{n}\right)^{2}\leq 2\frac{P_{m,t}^{n,\mathrm{loss}}}{\sqrt{2}\mathrm{A}^{\mathrm{sop}}}\frac{P_{m,t}^{n,\mathrm{loss}}}{\sqrt{2}\mathrm{A}^{\mathrm{sop}}} \tag{47}$$

$$\left(P_{m,t}^{n}\right)^{2}+\left(Q_{m,t}^{n}\right)^{2}\leq 2\frac{\mathrm{S}_{\mathrm{m}}^{\mathrm{n,sop}}}{\sqrt{2}}\frac{\mathrm{S}_{\mathrm{m}}^{\mathrm{n,sop}}}{\sqrt{2}} \tag{48}$$

The constraints for each bus's active and reactive power balance described in Eqs. (12) and (13) should be replaced by Eqs. (49) and (50).

$$P_{jt}^{in}+P_{m,t}^{n}+P_{m,t}^{\mathrm{loss}}=\sum_{k\in\varphi(j)}P_{jk,t}^{l}-\sum_{i\in\theta(j)}P_{ij,t}^{l} \tag{49}$$

$$Q_{jt}^{in}+Q_{m,t}^{n}=\sum_{k\in\varphi(j)}Q_{jk,t}^{l}-\sum_{i\in\theta(j)}Q_{ij,t}^{l} \tag{50}$$

Ultimately, SP1 is formulated as a MISOCP as follows:

$$\begin{aligned} &\min \sum_{m\in\mathrm{M}}C_{mg}^{m} \\ &\text{s.t. } (2)-(11),(14)-(19),(24)-(26), \\ &\quad (30)-(40),(43)-(44),(47)-(50) \end{aligned} \tag{51}$$

(2) SP2: Payment bargaining problem

The optimization model of SP2 is as follows:

$$\begin{aligned} &\max \prod_{m=1}^{\mathrm{M}}\left(C_{mg}^{m,\mathrm{ind}}-C_{mg}^{m,\mathrm{co}^{*}}-C_{m,mg}^{n,\mathrm{bar}}\right) \\ &\text{s.t. } C_{mg}^{m,\mathrm{ind}}-C_{mg}^{m,\mathrm{co}^{*}}-C_{m,mg}^{n,\mathrm{bar}}\geq 0 \\ &\quad C_{m,mg}^{n,\mathrm{bar}}+C_{n,mg}^{m,\mathrm{bar}}=0 \end{aligned} \tag{52}$$

where $C_{mg}^{m,\mathrm{ind}}$ is the cost of operating the MG m independently; $C_{mg}^{m,\mathrm{co}^{*}}$ is the operating cost of the MG m when P2P energy trading is conducted, $C_{m,mg}^{n,\mathrm{bar}}$ denotes the payment variable from MG m to MG n.

3.2. Decentralized solving method based on ADMM

In this paper, the SP1 and SP2 are solved in a distributed manner by using the ADMM algorithm to protect data privacy. To facilitate the description of the ADMM algorithm, a convex optimization problem is considered as follows:

$$\begin{aligned} &\min_{x\in S_x,y\in S_y} f(x)+g(y) \\ &\text{s.t.} \quad \mathrm{A}x+\mathrm{B}y=\mathrm{c} \end{aligned} \tag{53}$$

The augmented Lagrangian model of the convex optimization problem denotes as follows:

$$\begin{aligned} L_{\rho}(x,y,\lambda):=f(x)+g(y)+\lambda^{T}(Ax+By-c) \\ +\frac{\rho}{2}\|Ax+By-c\|_{2}^{2} \end{aligned} \tag{54}$$

where λ denotes Lagrangian multiplier, ρ is a positive constant. To apply the ADMM model, a three-step procedure could be defined in which the variables would be iteratively updated as below:

$$x^{k+1}=\arg\min_{x\in S_x}L_{\rho}\left(x,y^{k},\lambda^{k}\right) \tag{55}$$

$$y^{k+1}=\arg\min_{z\in S_z}L_{\rho}\left(x^{k},y,\lambda^{k}\right) \tag{56}$$

$$\lambda^{k+1}=\lambda^{k}+\rho\left(Ax^{k+1}+By^{k+1}-c\right) \tag{57}$$

Local variables x and global variables y update by using Eq. (55) and (56), respectively. Eq. (57) is used to update Lagrangian multiplier λ. Finally, the following criteria are defined in order to ensure convergence of the approach.

$$r^{k}:=\|Ax+By-c\| \tag{58}$$

$$s^{k}:=\rho\left\|A^{T}B\left(y^{k}-y^{k-1}\right)\right\| \tag{59}$$

where r^{k} represents primal residual, and s^{k} shows dual residual of the ADMM model.

The exact procedure for SP1 and SP2 using the ADMM algorithm is shown below.

(1) SP1: P2P energy trading problem

In SP1, Eq. (43) is the coupling constraint, which can be reformulated as Eqs. (60) and (61) by introducing auxiliary variables $\hat{P}_{m,t}^{n}$ and $\hat{P}_{m,t}^{\mathrm{loss}}$.

$$\hat{P}_{m,t}^{n}+\hat{P}_{m,t}^{\mathrm{loss}}+\hat{P}_{n,t}^{m}+\hat{P}_{n,t}^{\mathrm{loss}}=0 \tag{60}$$

$$P_{n,t}^{m}+P_{n,t}^{\mathrm{loss}}=\hat{P}_{n,t}^{m}+\hat{P}_{n,t}^{\mathrm{loss}} \tag{61}$$

The Lagrange multiplier of Eq. (61) is denoted by $\lambda_{1,m,t}^{n}$. Then, the augmented Lagrangian function about SP1 is expressed as:

$$\mathcal{L}_1 = \sum_{m\in \mathrm{M}} \mathcal{L}_{1,m}(\boldsymbol{x}^{\boldsymbol{m}}, \boldsymbol{y}^{\boldsymbol{m}}, \boldsymbol{\lambda}^{\boldsymbol{m}}) = \sum_{m\in \mathrm{M}} \left\{ C_{mg}^{m} + \sum_{t\in T} \sum_{n\in \mathrm{M}\setminus m} \left[\begin{array}{l} \lambda_{1,m,t}^{n}(P_{m,t}^{n} + P_{m,t}^{\mathrm{loss}} - \hat{P}_{n,t}^{m} - \\ \hat{P}_{n,t}^{\mathrm{loss}}) + \dfrac{\rho_1}{2} \left\| \begin{array}{l} P_{m,t}^{n} + P_{m,t}^{\mathrm{loss}} \\ -\hat{P}_{n,t}^{m} - \hat{P}_{n,t}^{\mathrm{loss}} \end{array} \right\| \end{array} \right] \right\} \quad (62)$$

where $\boldsymbol{x}^{\boldsymbol{m}}$ denotes the variables about MG m, $\boldsymbol{y}^{\boldsymbol{m}}$ denotes the auxiliary variable associated with MG m, and ρ_1 is the penalty factor of the quadratic term.

Based on the ADMM algorithm, using τ denotes the number of iterations, and the specific iterative solution process of SP1 is as follows [42].

Step 1 (initializing parameters): for each MG $m \in M$, initialize auxiliary variables $\boldsymbol{y}^{\boldsymbol{m}} = 0$ and $\boldsymbol{\lambda}^{\boldsymbol{m}} = 0$. Set the number of iterations $\tau = 0$, and the values of the convergence tolerance ς and penalty parameters ρ_1.

Step 2 (solving optimization models of each MG): due to the decomposability of the augmented Lagrangian function Eq. (62), each MG $m \in \mathrm{M}$ can solve its optimal scheduling problem independently. The optimization model of MG m can be expressed as follows:

$$\begin{aligned} \boldsymbol{x}^{m,\tau+1} := \arg\min\ & \mathcal{L}_{1,m}(\boldsymbol{x}^{m}, \boldsymbol{y}^{m,\tau}, \boldsymbol{\lambda}^{m,\tau}) \\ \text{s.t.}\ & (2)-(11), (14)-(19), (24)-(26), \\ & (30)-(40), (44), (47)-(50), (60) \end{aligned} \quad (63)$$

After solving Eq. (63), each MG $m \in \mathrm{M}$ broadcasts $P_{m,t}^{n,\tau+1}$ and $P_{m,t}^{\mathrm{loss},\tau+1}$ to MG n.

Step 3 (updating auxiliary variables): the auxiliary variables are updated according to Eq. (64).

$$\begin{aligned} \hat{P}_{m,t}^{n,\tau+1} + \hat{P}_{m,t}^{\mathrm{loss},\tau+1} &= -(\hat{P}_{n,t}^{m,\tau+1} + \hat{P}_{n,t}^{\mathrm{loss},\tau+1}) \\ &= \frac{(\hat{P}_{m,t}^{n,\tau+1} + \hat{P}_{m,t}^{\mathrm{loss},\tau+1}) - (\hat{P}_{n,t}^{m,\tau+1} + \hat{P}_{n,t}^{\mathrm{loss},\tau+1})}{2} \end{aligned} \quad (64)$$

Step 4 (updating Lagrange multipliers): each MG $m \in \mathrm{M}$ updates the Lagrange multiplier according to Eq. (65).

$$\lambda_{m,t}^{n,\tau+1} = \lambda_{m,t}^{n,\tau} + \rho_1 \begin{pmatrix} P_{m,t}^{n,\tau+1} + P_{m,t}^{\mathrm{loss},\tau+1} \\ -\hat{P}_{m,t}^{n,\tau+1} - \hat{P}_{m,t}^{\mathrm{loss},\tau+1} \end{pmatrix} \quad (65)$$

Step 5 (convergence judgement): the primal and dual residuals are calculated. When the residuals are less than the convergence tolerance, stop the iteration and output the optimization result, otherwise $\tau = \tau + 1$ and return to *Step 2*. The convergence criterion is specified in Eq. (66).

$$\max \begin{pmatrix} \left\| P_{m,t}^{n,\tau} + P_{m,t}^{loss,\tau} - \hat{P}_{m,t}^{n,\tau} - \hat{P}_{m,t}^{loss,\tau} \right\| \\ \left\| \hat{P}_{m,t}^{n,\tau} + \hat{P}_{m,t}^{loss,\tau} - \hat{P}_{m,t}^{n,\tau-1} - \hat{P}_{m,t}^{loss,\tau-1} \right\| \end{pmatrix} \le \varsigma \quad (66)$$

Remark: Global convergence of the ADMM algorithm can be guaranteed when the model is convex [43]. However, the model of SP1 is non-convex because of the binary variables. It has been verified in [44] that the ADMM algorithm can converge linearly in a finite number of iterations for the optimization model, including binary variables.

(2) SP2: Payment bargaining problem

Since the objective function of SP2 is non-convex, the problem cannot be solved directly. Firstly, the objective function of SP2 is reformulated into a convex function by logarithmic transformation. Then, similar to SP1, the auxiliary variable $\hat{C}_{m,mg}^{n,\mathrm{bar}}$ is introduced and the coupling constraint Eq. (52) is replaced by Eqs. (67) and (68).

$$\hat{C}_{m,mg}^{n,\mathrm{bar}} + \hat{C}_{n,mg}^{m,\mathrm{bar}} = 0 \quad (67)$$

$$C_{n,mg}^{m,\mathrm{bar}} = \hat{C}_{n,mg}^{m,\mathrm{bar}} \quad (68)$$

The Lagrange multiplier of Eq. (68) is denoted by $\lambda_{2,m,t}^{n}$. Then, the augmented Lagrangian function about SP2 is expressed as:

$$\mathcal{L}_2 = \sum_{m\in \mathrm{M}} \mathcal{L}_{2,m} = \sum_{m\in \mathrm{M}} \left\{ \begin{array}{l} -\ln\left(C_{mg}^{m,\mathrm{ind}} - C_{mg}^{m,\mathrm{co}^*} - C_{m,mg}^{n,\mathrm{bar}}\right) + \\ \sum\limits_{n\in \mathrm{M}\setminus m} \left[\begin{array}{l} \lambda_{2,m,t}^{n}\left(C_{n,mg}^{m,\mathrm{bar}} - \hat{C}_{n,mg}^{m,\mathrm{bar}}\right) \\ + \dfrac{\rho_2}{2} \left\| C_{n,mg}^{m,\mathrm{bar}} - \hat{C}_{n,mg}^{m,\mathrm{bar}} \right\| \end{array} \right] \end{array} \right\} \quad (69)$$

Afterward, SP2 is solved iteratively using the same steps described in SP1, which are not repeated here. The overall process flowchart of the method proposed in this paper is illustrated in Fig. 2.

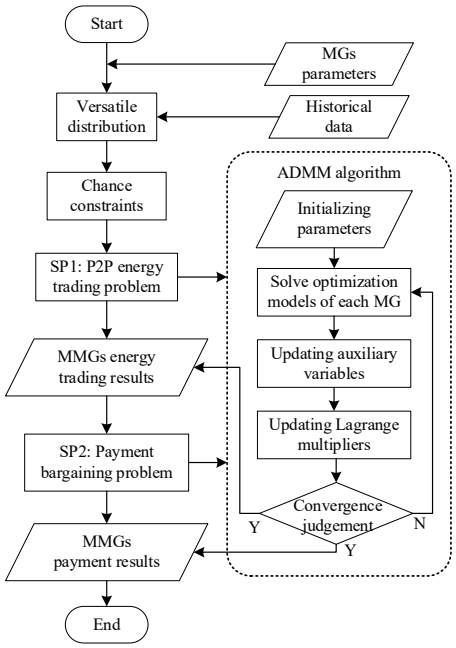

Fig. 2. Flowchart of the proposed method.

4. Case study

4.1. System Configuration

In this paper, based on the IEEE 123-bus distribution network [45], MMG containing three MGs is constructed, as shown in Fig. 3. The hourly electricity prices of the main grid are shown in Fig. 4 [46]. The base values of load consumption

in MG1, MG2, and MG3 are 1.47 MW, 1.75 MW, and 2.15 MW, respectively. The PV and WT installed capacities at each bus are 0.65 MW and 0.55 MW, respectively. The hourly forecasting power curves of load, PV, and WT in three MGs are the same, as shown in Fig. 5. The equipment parameters in the three MGs are the same, as shown in Table 2 [47]. The convergence tolerance ς is 10^{-4}. The confidence level ε is 0.95. The code is programmed in Matlab and solved by Mosek.

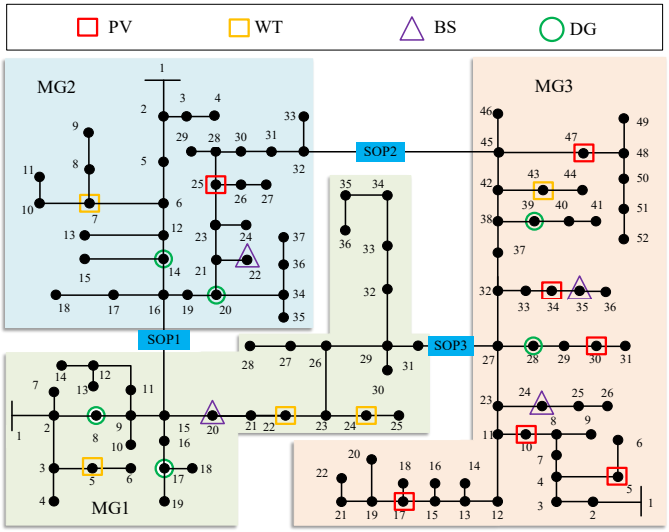

Fig. 3. A MMG containing three MGs adapted from the IEEE 123-bus distribution network.

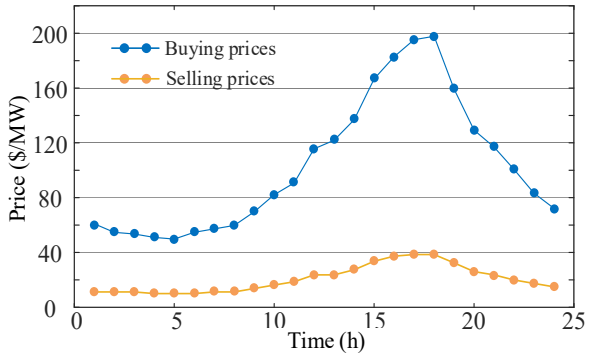

Fig. 4. Hourly electricity prices of the main grid.

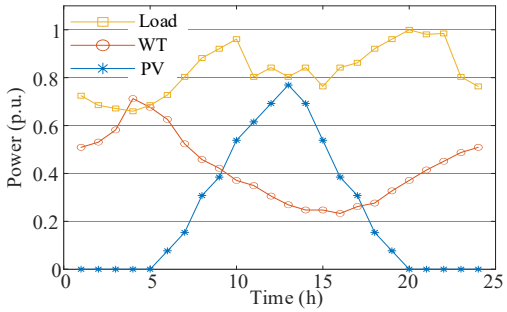

Fig. 5. Hourly forecasting power curves of load, PV, and WT.

Table 2

Equipment parameters of the three MGs.

Parameters	Value	Parameters	Value
a_g	200 ($/MWh^2)	$\overline{Q}_{gd}$	2 MVAR
b_g	116.7 ($/MWh)	$\underline{E}^{bs}$	0.06 MWh
c_g	0	$\overline{E}^{bs}$	0.54 MWh
$pr^{g,su}$	10 $	E_0^{bs}	0.3 MWh
$pr^{g,dn}$	6 $	$\overline{P}^{bs,c}$ / $\overline{P}^{bs,d}$	0.2 MW
$\underline{P}^{g}$	0.04 MW	η^{c}	0.95
$\overline{P}^{g}$	0.4 MW	η^{d}	0.95
V_0	1	$S_m^{n,sop}$	2 MVA
$\Delta\overline{V}$	0.05	A^{sop}	0.02
$\overline{P}^{gd}$	2 MW	$\overline{Q}_m^{n,sop}$	0.7 MVAR

4.2. Results and Analysis

(1) Fitting results of versatile distribution

This section analyzes the superiority of the versatile distribution utilized in this paper for capturing the probability distribution of forecasting errors. We assume that the forecast error of load consumption follows the Gaussian distribution. The forecast error distributions of WT and PV are assumed with positive and negative skewness, respectively. Monte Carlo simulation is used to generate the historical forecast error data. The forecast deviation is defined as the forecast error divided by the forecast value. Distribution parameters of the forecast deviation are shown in Table 3. The results of shape parameters obtained by the nonlinear least-squares fitting method are shown in Table 4. The CDF results of versatile distribution are shown in Fig. 6.

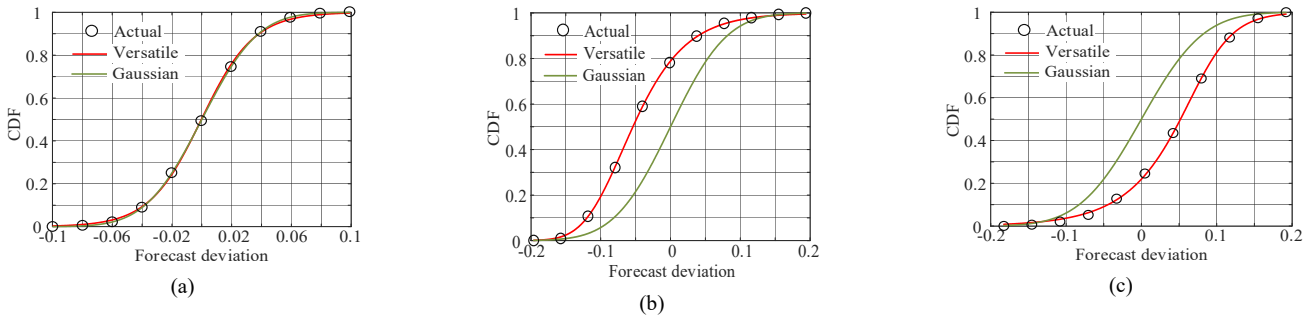

Fig. 6. CDF results of versatile distribution (a) Load (b) WT (c) PV.

Table 3

Distribution parameters of the forecast deviation.

	Mean	Variance	Skew	Kurtosis
Load	0	0.0009	0	3
PV	0.0405	0.0047	-0.667	0.5098
WT	-0.0405	0.0047	0.667	0.5098

Table 4

Results of shape parameters.

	δ	β	γ
Load	57.01	1.0208	-0.0005
PV	36.8185	0.4657	0.0841
WT	19.5104	4.5218	-0.1423

As shown in Fig. 6, the CDF of the historical forecast errors can be well fitted using the versatile distribution regardless of whether the actual historical forecast error data follow the Gaussian distribution. Hence, by employing the versatile distribution proposed in this paper as the foundation of formulating chance constraints, the obtained scheduling strategy becomes better aligned with confidence level requirement of chance constraints.

(2) Scheduling results of energy and reserve

Based on the results of solving the SP1, the operation cost of three MGs in each iteration are shown in Fig. 7. In terms of computational complexity, adopting the data-driven CCP approach proposed in this paper only requires adding constraints (30) – (37) to the determined optimization problem. Since these constraints are all linear, they impose a minimal burden on solving the problem. The simulations were conducted using a laptop with a 2.3 GHz Intel i7 CPU. As shown in Fig. 7, convergence is achieved after 17 iterations. Moreover, considering that each MGO can independently solve its optimization problem in parallel, the required solution time is only 12 seconds, demonstrating high computational efficiency.

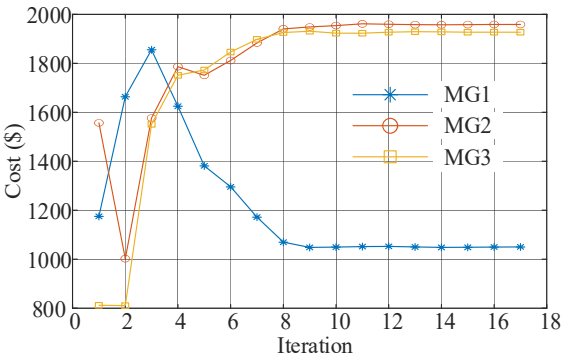

Fig. 7. Operation costs of three MGs in each iteration.

The energy and reserve dispatch results of each MG are shown in Fig. 8 and Fig. 9, respectively.

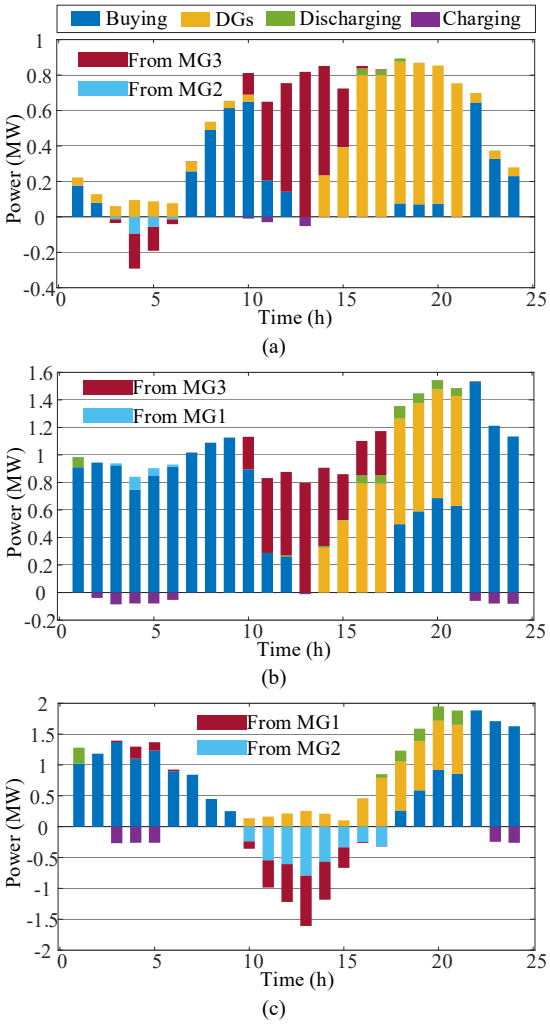

Fig. 8. Energy dispatch results (a) MG1 (b) MG2 (c) MG3.

As shown in Fig. 8, the MGs purchase electricity from the main grid and charge the BSs when the buying price is lower. In contrast, the MGs turn on the DGs and discharge the BSs when higher buying price. Besides, during hours 4 and 5, the energy surplus of MG1 is transmitted to the MG2 and MG3 via SOPs. Due to the high installed PV capacity in MG3, the surplus PV generation in MG3 is transmitted to MG1 and MG2 in hours 10–17. It can be seen that the MGs do not sell electricity to the grid, which implies that MGs prefer P2P trading to reduce the total operating cost of MMG, rather than the transaction with the main grid. The local utilization of renewable energy is also improved by P2P trading.

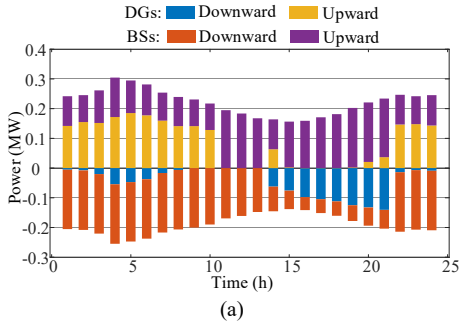

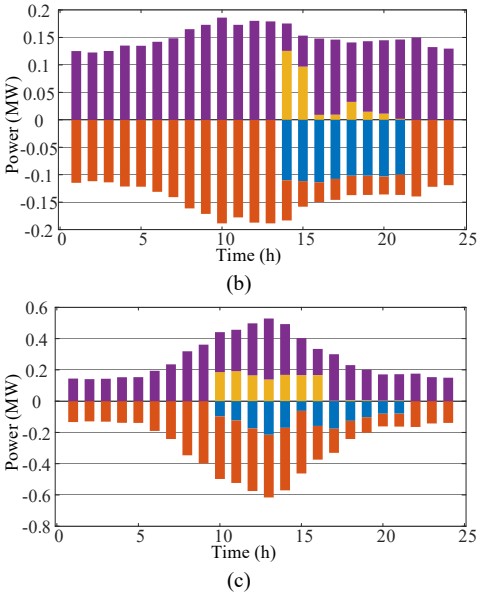

Fig. 9. Reserve dispatch results (a) MG1 (b) MG2 (c) MG3.

As shown in Fig. 9, the upward and downward reserves of DGs and BSs are dispatched day-ahead to balance the forecast errors of uncertain variables.

(3) Nash bargaining results of MMG

After a total of 16 iterations, SP2 reaches convergence, demonstrating the high computational efficiency of the ADMM algorithm used in this paper. The computation time of both SP1 and SP2 is found to be well within acceptable limits for the day-ahead scheduling problem. The bargaining results among the three MGs are obtained and presented in Table 5.

Table 5

Operating cost of each MG.

Cost ($)	Independent operation	P2P operation	
		Before bargaining	After bargaining
MG1	1359.02	1048.1	1178.07
MG2	2397.05	1959.94	2215.7
MG3	1711.7	1917.32	1531.6
Total cost	5467.77	4925.36	4925.37

In Table 5, the before bargaining operating cost of MG3 is increased compared to the cost when operating individually. When the MMG perform P2P transactions, the surplus energy in MG3 is transmitted to other MGs instead of selling to the main grid. Thus, the operating costs of MG1 and MG2 are reduced, and the revenue of MG3 from electricity sales is reduced. After bargaining, the total benefit by P2P trading is distributed to all the MGs in the MMG. After bargaining the costs of all the MGs are reduced compared to the costs when operating independently. The total operating costs of the three MGs are 5467.77 $ and 4925.37 $ in the independent and P2P operation modes, respectively. Due to P2P trading, the total operating cost of the MMG is reduced by 9.92%. When P2P trading is executed in the centralized scheduling framework, the total operating cost of the three MGs is 4924.77 $. It can be seen that the difference between the distributed and centralized solutions is only 0.0122%, which verifies the effectiveness of the ADMM algorithm.

(4) The impact of network constraints

In this section, three cases have been designed to demonstrate through comparative analysis that the proposed method in this paper exhibits superiority in adhering to the network constraints within the microgrid system while formulating P2P energy strategies. Case 1: the network constraints of MGs are not considered, Case 2: the network constraints are considered without the chance constraints for the limit of bus voltage, Case 3: the network chance constraints of MGs are considered with the chance constraints for the limitation of bus voltage. The results of bus voltage of the MMG in the three Cases are shown in Fig. 10.

As shown in Fig. 10(a), in Case 1, the voltage of MGs in 22–24 hours violate the lower bound due to the negligence of network constraints. This is because the load consumption is high, and DGs are not operating in 22–24 hours, causing under-voltage violations at the end buses in MG2 and MG3. In Case 2, when the network constraints are considered, the lower bound constraint of the bus voltage is satisfied, as shown in Fig. 10(b). In Case 3, when the network chance constraints are considered, the minimum values of the buses voltage in 22–24 hours are further increased, as shown in Fig. 10(c). This provides a downward adjustment margin to ensure that the network constraints are still satisfied when the reserve is scheduled to balance the forecast errors at the real-time stage.

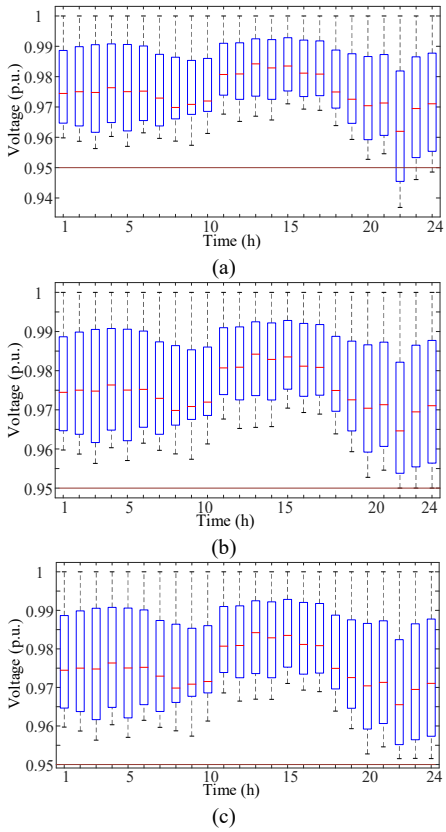

Fig. 10. Results of MMG bus voltage (a) Case 1 (b) Case 2 (c) Case 3.

In fact, the network constraints of the MMG are satisfied by SOP2 generating reactive power to MG2 and MG3 in Cases 2

and 3. The specific results of the reactive power generated by SOP2 at 22–24 hours in three Cases are shown in Fig. 11.

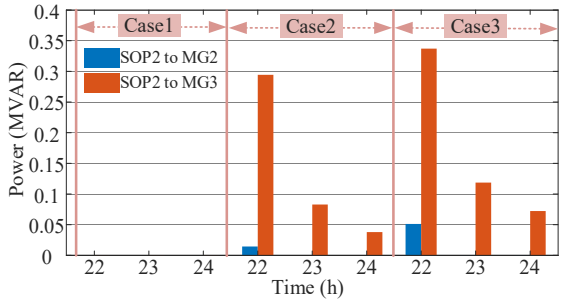

Fig. 11. Results of the reactive power generated by SOP2 at 22–24 hours.

In Case 1, since the network constraints of the MMG are not considered, SOP2 does not output reactive power, which causes the bus voltage violates the lower bound, as shown in Fig. 10(a). In Cases 2 and 3, SOP2 generates reactive power to MG2 and MG3 at 22 hours and 22-24 hours, respectively, for increasing the voltage magnitude at the end buses to satisfy the network constraint of the MMG. In addition, SOP2 outputs more reactive power in Case 3 than in Case 2. This is because in Case 3, SOP2 needs to generate more reactive power to increase the bus voltage amplitude further to meet the chance constraint for the limitation of bus voltage.

The operating cost of MGs in the three Cases are shown in Table 6.

Table 6
Operating cost in the three Cases.

Cost ($)	Case 1	Case 2	Case 3
MG1	1177.86	1178.15	1178.07
MG2	2215.75	2216.07	2215.69
MG3	1529.57	1530.63	1531.60
Total cost	4923.19	4924.85	4925.36

As shown in Table 6, there are only slight differences in the operating costs of MGs in the three Cases. In Cases 2 and 3, the network constraints of the MMG are satisfied through the reactive power output of SOP2, and they do not affect the P2P energy (i.e., active power) trading results between MGs. In addition, the total cost of Case 2 increases slightly compared to Case 1, and the total cost of Case 3 increases compared to Case 2. This is because the increased output reactive power of SOP2 results in more active power losses, leading to a slightly higher total cost for the MMG. It is worth noting that while the economic outcomes of P2P energy trading among MMG show only minimal differences across the three cases, the scheduling results for Cases 1 and 2, in fact, fail to meet the MGO's operational constraints. In contrast, the scheduling results obtained in Case 3 effectively satisfy the MGO's operational constraints while considering prediction errors, showcasing the superiority of the method proposed in this paper.

(5) The impact of confidence level

The changes in reserve demand and operating costs of the MMG with various confidence levels are shown in Fig. 12 and Fig. 13, respectively.

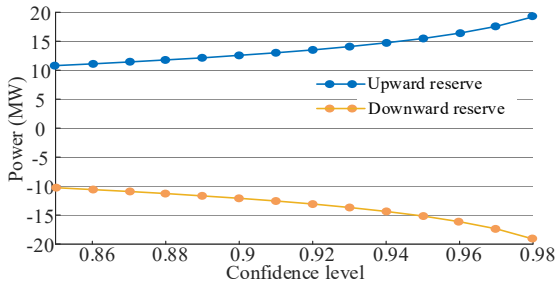

Fig. 12. The reserve demand of the MMG.

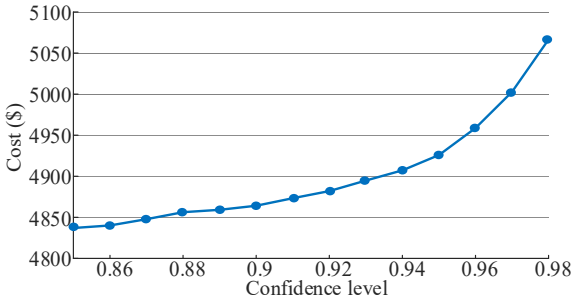

Fig. 13. The operating costs of the MMG.

In Fig. 12, as the confidence level increases, the MMG require more upward and downward reserve demand to satisfy the chance constraints. Correspondingly, the operating costs of the MMG also increase with the confidence level, as shown in Fig. 13. This increase is due to the reduction in day-ahead dispatchable flexibilities of DGs and BSs, coupled with the need for additional reserves. By choosing the appropriate confidence level, operators can control the conservativeness of the day-ahead dispatch strategy.

5. Conclusion

In this paper, a decentralized P2P energy trading strategy for a MMG is proposed. Firstly, the practical network constraints within the MGs are taken into consideration, and a joint energy and reserve economic dispatch model is established for an individual MG. In response to forecast errors of renewable energy generation and load demand, chance constraints regarding bus voltages and reserve capacity limits have been introduced. To meet the confidence level of chance constraints more accurately, the probability distribution characteristics of forecast errors have been captured using the versatile distribution in a data-driven manner. This approach avoids making premature assumptions about the probability distribution. Then, an interconnected MMG is constructed using SOPs. Nash bargaining game theory is then utilized to establish the P2P energy trading model for the MMG. Furthermore, this model is equivalently decomposed into two sub-problems: the P2P energy trading problem and the payment bargaining problem, which are solved in sequence. Moreover, to ensure the data privacy of MGOs, the ADMM algorithm is adopted to solve the two sub-problems. By employing the method proposed in this paper to

formulate P2P energy trading strategies in an MMG, the operational costs of the MMG are reduced. Simultaneously, all MGs can benefit from P2P energy trading, and the obtained risk-averse scheduling result can effectively adhere to internal network constraints, mitigating the impact of forecast errors on MG operating limitations.

MMG containing three MGs is constructed based on the IEEE 123-bus distribution network for simulation. The results show that the operating costs of the MMG decreases by 9.92% and reasonable distribution of total benefits among MGs is achieved. Hence, each MG has sufficient incentives to participate in P2P trading. In addition, the economic schedules of energy and reserve for each MG are obtained while ensuring the robustness of reserve capacity and bus voltage constraints against forecast errors. Finally, the impacts of confidence level on reserve demand and operating costs are analyzed.

This paper focuses on energy trading between MGs, and the optimal P2P trading strategy of both energy and reserve can be further studied in the future. Moreover, the optimal design and planning of MMG is a promising topic that can also be explored in future research.

Acknowledgment

This work was supported by the Key Research and Development Program of Tianjin (No. 20YFYSGX00060).

Reference

[1] Aguila-Leon J, Vargas-Salgado C, Chiñas-Palacios C, Díaz-Bello D. Energy management model for a standalone hybrid microgrid through a particle Swarm optimization and artificial neural networks approach. Energy Conversion and Management 2022; 267: 115920.

[2] Xu Z, Yang P, Zheng C, Zhang Y, Peng J, Zeng Z. Analysis on the organization and development of multi-microgrids. Renewable and Sustainable Energy Reviews 2018; 81:2204–2216.

[3] Ng E, El-Shatshat R. Multi-microgrid control systems (MMCS), in Proc. IEEE Power Eng. Soc. Gen. Meeting, Minneapolis, MN, USA, Jul. 2010, pp. 1–6.

[4] Zhang B, Hu W, Ghias A M Y M, Xu X, Chen Z. Multi-agent deep reinforcement learning based distributed control architecture for interconnected multi-energy microgrid energy management and optimization. Energy Conversion and Management 2023; 277: 116647.

[5] Hutty T D, Pena-Bello A, Dong S, Parra D, Rothman R, et al. Peer-to-peer electricity trading as an enabler of increased PV and EV ownership. Energy Conversion and Management 2021; 245: 114634.

[6] Vand B, Ruusu R, Hasan A, Delgado B M. Optimal management of energy sharing in a community of buildings using a model predictive control. Energy Conversion and Management 2021; 239: 114178.

[7] Nikmehr N, Ravadanegh S. Optimal power dispatch of multi-microgrids at future smart distribution grids. IEEE Transactions on Smart Grid 2015; 6(4): 1648–1657.

[8] Ouammi A, Dagdougui H, Sacile R. Optimal control of power flows and energy local storages in a network of microgrids modeled as a system of systems. IEEE Transactions on Control Systems Technology 2014; 23(1): 128–138.

[9] Qu ZL, Chen JJ, Peng K, Zhao YL, Rong ZK, Zhang MY. Enhancing stochastic multi-microgrid operational flexibility with mobile energy storage system and power transaction. Sustainable Cities and Society 2021; 71: 102962.

[10] Bahmani R, Karimi H, Jadid S. Stochastic electricity market model in networked microgrids considering demand response programs and renewable energy sources. International Journal of Electrical Power & Energy Systems 2020; 117: 105606.

[11] Li Y, Zhao T, Wang P, Gooi HB, Wu L, Liu Y. Optimal operation of multimicrogrids via cooperative energy and reserve scheduling. IEEE Transactions on Industrial Informatics 2018; 14(8): 3459–3468.

[12] Li G, Li Q, Liu Y, Liu H, Song W, Ding R. A cooperative Stackelberg game based energy management considering price discrimination and risk assessment. International Journal of Electrical Power & Energy Systems 2022; 135: 107461.

[13] Jafari A, Ganjehlou H, Khalili T, Bidram A. A fair electricity market strategy for energy management and reliability enhancement of islanded multi-microgrids. Applied Energy 2020; 270: 115170.

[14] Wang Z, Chen B, Wang J, Begovic MM, Chen C. Coordinated energy management of networked microgrids in distribution systems. IEEE Transactions on Smart Grid 2014; 6(1): 45–53.

[15] Kong X, Liu D, Wang C, Sun F, Li S. Optimal operation strategy for interconnected microgrids in market environment considering uncertainty. Applied Energy 2020; 275: 115336.

[16] Wang H, Huang J. Incentivizing energy trading for interconnected microgrids. IEEE Transactions on Smart Grid 2016; 9(4): 2647–2657.

[17] Kim H, Lee J, Bahrami S, Wong VW. Direct energy trading of microgrids in distribution energy market. IEEE Transactions on Power Systems 2019; 35(1): 639–651.

[18] Xuanyue S, Wang X, Wu X, Wang Y, Song Z, Wang B, et al. Peer-to-peer multi-energy distributed trading for interconnected microgrids: A general Nash bargaining approach. International Journal of Electrical Power & Energy Systems 2022; 138: 107892.

[19] Zhong X, Zhong W, Liu Y, Yang C, Xie S. Optimal energy management for multi-energy multi-microgrid networks considering carbon emission limitations. Energy 2022; 246: 123428.

[20] Hu B, Gong Y, Chung C, Noble BF, Poelzer G. Price-maker bidding and offering strategies for networked microgrids in day-ahead electricity markets. IEEE Transactions on Smart Grid 2021; 12(6): 5201–5211.

[21] Saatloo A M, Mirzaei M A, Mohammadi-Ivatloo B. A robust decentralized peer-to-peer energy trading in community of flexible microgrids. IEEE Systems Journal, 2022; 17(1): 640-651.

[22] Zou Y, Xu Y, Feng X, et al. Peer-to-peer transactive energy trading of a reconfigurable multi-energy network. IEEE Transactions on Smart Grid, 2022; 14(3): 2236-2249.

[23] Li P, Ji H, Wang C, Zhao J, Song G, Ding F, et al. Optimal operation of soft open points in active distribution networks under three-phase unbalanced conditions. IEEE Transactions on Smart Grid 2017; 10(1): 380–391.

[24] Li J, Khodayar M, Wang J, Zhou B. Data-driven distributionally robust co-optimization of P2P energy trading and network operation for interconnected microgrids. IEEE Transactions on Smart Grid 2021; 12(6): 5172–5184.

[25] Liu Y, Li Y, Gooi H, Jian Y, Xin H, Jiang X. Distributed robust energy management of a multimicrogrid system in the real-time energy market. IEEE Transactions on Sustainable Energy 2017; 10(1): 396–406.

[26] Wei C, Shen Z, Xiao D, Wang L, Bai X, Chen H. An optimal scheduling strategy for peer-to-peer trading in interconnected microgrids based on RO and Nash bargaining. Applied Energy 2021; 295: 117024.

[27] Li Y, Wang C, Li G, Wang J, Zhao D, et al. Improving operational flexibility of integrated energy system with uncertain renewable generations considering thermal inertia of buildings. Energy Conversion and Management 2020; 207: 112526.

[28] Matamala Y, Feijoo F. A two-stage stochastic Stackelberg model for microgrid operation with chance constraints for renewable energy generation uncertainty. Applied Energy 2021; 303: 117608.

[29] Zhao J, Zhang M, Yu H, Ji H, Song G, Li P, et al. An islanding partition method of active distribution networks based on chance-constrained programming. Applied Energy 2019; 242: 78–91.

[30] Chen S, Li P, Ji H, Yu H, Yan J, Wu J, et al. Operational flexibility of active distribution networks with the potential from data centers. Applied Energy 2021; 293: 116935.

[31] Baran ME, Wu FF. Network reconfiguration in distribution systems for loss reduction and load balancing. IEEE Power Engineering Review 1989; 9(4): 101–102.

[32] Wang Z, Chen B, Wang J, Kim J, Begovic M. Robust optimization based optimal DG placement in microgrids. IEEE Transactions on Smart Grid 2014; 5(5): 2173–2182.

[33] Zhang Z, Sun Y, Gao D, Lin J, Cheng L. A versatile probability distribution model for wind power forecast errors and its application in economic dispatch. IEEE Transactions on Power Systems 2013; 28(3): 3114–3125.

[34] Wang X, Li F, Dong J, Olama M, Zhang Q, Shi Q. Tri-level scheduling model considering residential demand flexibility of aggregated HVACs and EVs under distribution LMP. IEEE Transactions on Smart Grid 2021; 12(5): 3990–4002.
[35] Wang L, Zhu Z, Jiang C, Li Z. Bi-level robust optimization for distribution system with multiple microgrids considering uncertainty distribution locational marginal price. IEEE Transactions on Smart Grid 2020; 12(2): 1104–1117.
[36] Wu X, Qi S, Wang Z, Duan C, Wang X, Li F. Optimal scheduling for microgrids with hydrogen fueling stations considering uncertainty using data-driven approach. Applied Energy 2019; 253: 113568.
[37] Wang J, Zhong H, Tang W, Rajagopal R, Xia Q, Kang C, et al. Optimal bidding strategy for microgrids in joint energy and ancillary service markets considering flexible ramping products. Applied Energy 2017; 205: 294–303.
[38] Erenoğlu A, Şengör İ, Erdinç O, Taşcıkaraoğlu A, Catalão J. Optimal energy management system for microgrids considering energy storage, demand response and renewable power generation. International Journal of Electrical Power & Energy Systems 2022; 136: 107714.
[39] Thang V, Ha T, Li Q, Zhang Y. Stochastic optimization in multi-energy hub system operation considering solar energy resource and demand response. International Journal of Electrical Power & Energy Systems 2022; 141: 108132.
[40] Wu X, Li H, Wang X, Zhao W. Cooperative operation for wind turbines and hydrogen fueling stations with on-site hydrogen production. IEEE Transactions on Sustainable Energy 2020; 11(4): 2775–2789.
[41] Wang J, Zhou N, Chung CY, Wang Q. Coordinated planning of converter-based DG units and soft open points incorporating active management in unbalanced distribution networks. IEEE Transactions on Sustainable Energy 2019; 11(3): 2015–2027.
[42] Chen H, Zhang Y, Zhang R, Lin C, Jiang T, et al. Privacy-preserving distributed optimal scheduling of regional integrated energy system considering different heating modes of buildings. Energy Conversion and Management 2021; 237: 114096.
[43] Boyd S, Parikh N, Chu E, Peleato B, Eckstein J. Distributed optimization and statistical learning via the alternating direction method of multipliers. Foundations and Trends in Machine learning 2011; 3(1): 1–122.
[44] Mohiti M, Monsef H, Anvari-Moghaddam A, Guerrero J, Lesani H. A decentralized robust model for optimal operation of distribution companies with private microgrids. International Journal of Electrical Power & Energy Systems 2019; 106: 105–123.
[45] IEEE PES AMPS DSAS Test Feeder Working Group Distribution Test Feeders. http://sites.ieee.org/pestestfeeders/resources; 2022 [accessed 15 March 2022].
[46] Yan M, Shahidehpour M, Paaso A, Zhang L, Alabdulwahab A, Abusorrah A. Distribution network-constrained optimization of peer-to-peer transactive energy trading among multi-microgrids. IEEE Transactions on Smart Grid 2020; 12(2): 1033–1047.
[47] Wu Y, Lim G J, Shi J. Stability-constrained microgrid operation scheduling incorporating frequency control reserve. IEEE Transactions on Smart Grid, 2019; 11(2): 1007–1017.